

# Unconventional Cavity Optomechanics: Nonlinear Control of Phonons in the Acoustic Quantum Vacuum

Xin Wang,<sup>1,2</sup> Wei Qin,<sup>2</sup> Adam Miranowicz,<sup>2,3</sup> Salvatore Savasta,<sup>2,4</sup> and Franco Nori<sup>2,5</sup>

<sup>1</sup>*Institute of Quantum Optics and Quantum Information,  
School of Science, Xi'an Jiaotong University, Xi'an 710049, China*

<sup>2</sup>*Theoretical Quantum Physics Laboratory, RIKEN Cluster for Pioneering Research, Wako-shi, Saitama 351-0198, Japan*

<sup>3</sup>*Faculty of Physics, Adam Mickiewicz University, 61-614 Poznań, Poland*

<sup>4</sup>*Dipartimento di Scienze Matematiche e Informatiche, Scienze Fisiche e Scienze della Terra,  
Università di Messina, I-98166 Messina, Italy*

<sup>5</sup>*Physics Department, The University of Michigan, Ann Arbor, Michigan 48109-1040, USA*

(Dated: February 27, 2019)

We study unconventional cavity optomechanics and the acoustic analogue of radiation pressure to show the possibility of nonlinear coherent control of phonons in the acoustic quantum vacuum. Specifically, we study systems where a quantized optical field effectively modifies the frequency of an acoustic resonator. We present a general method to enhance such a nonlinear interaction by employing an intermediate qubit. Compared with conventional optomechanical systems, the roles of mechanical and optical resonators are interchanged, and the boundary condition of the phonon resonator can be modulated with an ultrahigh optical frequency. These differences allow to test some quantum effects with parameters which are far beyond the reach of conventional cavity optomechanics. Based on this novel interaction form, we show that various nonclassical quantum effects can be realized. Examples include an effective method for modulating the resonance frequency of a phonon resonator (e.g., a surface-acoustic-wave resonator), demonstrating mechanical parametric amplification, a nonlinear photon-phonon transducer, Kerr-coupler, and the dynamical Casimir effect of phonons originating from the acoustic quantum vacuum. Our results demonstrate that unconventional optomechanics offers a versatile hybrid platform for quantum engineering of nonclassical phonon states in quantum acoustodynamics.

Optomechanical systems [1, 2], in which quantized optical fields interact with a massive movable mirror via radiation pressure, bring together quantum physics and the macroscopic classical world. The basic mechanism of optomechanics is that the position of a movable mirror produces a time-dependent boundary condition of quantized electromagnetic fields, which in turn modulate an effective cavity resonant frequency [3]. Optomechanical systems provide a versatile platform to examine fundamental concepts of quantum physics and explore the classical-quantum boundary. Examples include testing wave-function-collapse models [4–6], studying the dynamical Casimir effect (DCE) [7–15], and putting massive objects into nonclassical states [16, 17]. One may wonder whether there are unconventional optomechanical (UOM) systems, where the *boundary condition of a mechanical resonator can be changed by a quantized optical field*. We show that such UOM systems can indeed exist, and give a general method to produce an UOM nonlinear interaction for controlling phonons (i.e., quantum engineering of phonons). In particular, we show how to realize: (i) a mechanical phase-sensitive amplifier, (ii) photon-phonon Kerr interaction, and (iii) an acoustic analogue of optical DCE. The acoustic DCE tries to simulate cosmological phenomena such as Hawking radiation and the Unruh effect [18–21]. However, no experiment has shown the phonon DCE using a phonon resonator at the quantum level: i.e., the effects where quantized photons are converted into DCE

pairs of itinerant phonons.

Let us recall the interaction form in a conventional optomechanical (COM) system. Setting  $\hbar = 1$ , an exact form of the interaction Hamiltonian between a single-mode optical field and a moving mirror is  $H_{\text{COM}} = G_{\text{COM}}(a + a^\dagger)^2(b + b^\dagger)$  [3], where  $a$  and  $b$  ( $a^\dagger$  and  $b^\dagger$ ) are the annihilation (creation) operators of the optical and mechanical modes, respectively; and the single-photon coupling strength is  $G_{\text{COM}}$ . Note that in most studies, the quadratic terms  $a^2$  and  $a^{\dagger 2}$  are often neglected, because they describe rapidly oscillating virtual processes where photons are annihilated and created in pairs. As a result, the COM interaction,  $H'_{\text{COM}} = 2G_{\text{COM}}a^\dagger a(b + b^\dagger)$ , is obtained.

We start our discussion of an UOM system by considering classical mechanical parametric amplification (MPA), where the spring constant  $k[E(t)]$  of a mechanical oscillator is modulated with a time-dependent field  $E(t)$  [22–25]. As depicted in Fig. 1(a), we consider that the amplification source is not a classical drive, but a quantized electromagnetic field,  $E(t) = \varepsilon_0(a + a^\dagger)$ , oscillating at frequency  $\omega_c$ , where  $\varepsilon_0$  is the zero-point fluctuation. Expanding the potential term of the mechanical mode to first order in  $E(t)$ , we obtain the interaction term as [22]:

$$V(t) = \frac{1}{2}k[E(t)]x^2 \simeq \frac{1}{2}k_0x^2 + \frac{1}{2}RE(t)x^2, \quad (1)$$

where  $k_0$  is the spring constant without the modulating field,  $E(t) = 0$ , and  $x = x_0(b + b^\dagger)$  is the

mechanical position operator with  $x_0$  being the zero-point fluctuation. The last term in Eq. (1), describes the response of the spring constant to the optical field with sensitivity  $R = (\partial k(E)/\partial E)|_{E(t)=0}$ , and can be rewritten as

$$H_{\text{UOM}} = G_{\text{UOM}}(b + b^\dagger)^2(a + a^\dagger), \quad (2)$$

where  $G_{\text{UOM}} = R\varepsilon_0 x_0^2/2$  is the nonlinear coupling strength. Compared with the COM Hamiltonian,  $H_{\text{UOM}}$  has the inverse form, where the roles of the mechanical oscillator and optical field are interchanged. We can interpret  $H_{\text{UOM}}$  as a phonon intensity effectively inducing “motions” of the optical field, with a mechanism which is analogous to that of COM.

The UOM interaction requires that the spring constant linearly responds to a fast-oscillating quantized electric field. To observe the coherence effects, this response should be ultra-sensitive (a large  $R$ ) to enable a strong coupling strength  $G_{\text{UOM}}$ . Obtaining such large  $R$  is still challenging in conventional MPA experiments. For example, in Ref. [25], the spring constant is modulated by an external voltage via the piezoelectric effect, and the sensitivity  $R$  is about 40 kHz/V. We assume that the quantized bias voltage is provided by a microwave transmission-line resonator (TLR), where the typical zero-point voltage fluctuation is  $\sim 0.1\text{--}1\ \mu\text{V}$  [26]. The single-phonon UOM coupling strength is  $G_{\text{UOM}} \simeq 10^{-2}\text{--}10^{-3}\ \text{Hz}$ , which is too weak to produce observable coherent effects. Alternatively, one can effectively simulate the UOM interaction in a membrane-in-middle optomechanical system [27, 28]. Since the effective UOM interaction results from higher-order terms of the quadratic optomechanical coupling, the interaction strength is also very weak. So far, no proposal has discussed how to realize a real UOM with strong enough strength for quantum-optical engineering.

*Qubit-mediated UOM coupling.*—Both optical and mechanical oscillators are linear bosonic systems. Single-phonon-photon nonlinear interactions (e.g., the COM coupling) are usually much weaker than conventional light-matter interactions [29, 30]. To increase their nonlinear interactions, one possible method is to introduce nonlinear elements. For example, a Josephson-junction-based qubit can help to induce a strong COM interaction [31, 32].

Concerning nonlinearity, a qubit is naturally a highly nonlinear system. By exploiting this nonlinearity, one may enhance the UOM interaction to an observable level. To introduce our idea, we consider that a mechanical oscillator *transversely* interacts with a qubit. The interaction Hamiltonian is  $H_{\text{qm}} = g_x \sigma_x (b + b^\dagger)$ , where  $g_x$  is the coupling strength, while  $\sigma_z = |e\rangle\langle e| - |g\rangle\langle g|$  and  $\sigma_x = |e\rangle\langle g| + |g\rangle\langle e|$  are the qubit Pauli operators with  $|g, e\rangle$  being the qubit ground and excited states. Naturally, a dispersive coupling between them is induced,

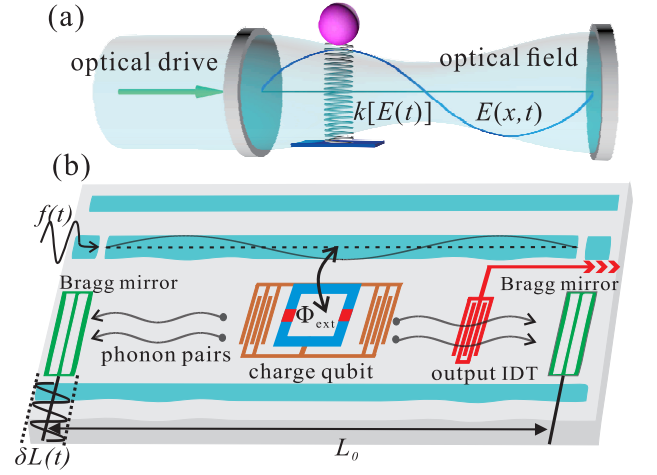


FIG. 1. (a) Diagrammatic sketch of an unconventional optomechanical (UOM) system: A localized mechanical oscillator (with a massive particle) is placed inside an optical cavity, and its spring constant is linearly modulated by the cavity quantized field  $E(x, t)$ . (b) UOM system based on a surface-acoustic-wave (SAW) resonator: A charge-qubit, with two Josephson junctions (red bars) is placed into the SAW resonator (confined by two Bragg mirrors). Their interaction is mediated via two identical inter-digitated-transducers (IDTs) of capacitance  $C_q$  via the piezoelectric effects. A transmission-line resonator (TLR) longitudinally couples to the charge-qubit via the mutual inductance  $M$ . The field current operator  $\dot{I}(t)$  effectively changes the SAW resonator length  $L$  by amount  $\delta L(t)$ . One Bragg mirror acts as a fast “oscillating” mirror.

i.e.,  $H_0^{\text{dis}} = \chi(b^\dagger + b)^2 \sigma_z$ , with  $\chi \simeq g_x^2/\omega_q$ . Different from the conventional dispersive coupling form,  $H_0^{\text{dis}}$  includes the additional quadratic terms  $b^{\dagger 2}$  and  $b^2$ , which result from the counter-rotating terms in  $H_{\text{qm}}$  [33].

The optical cavity is involved in this hybrid system by considering its *longitudinal* coupling to the qubit with strength  $g_z$  [34–37]. The interaction Hamiltonian reads  $H_{\text{qc}} = g_z \sigma_z (a + a^\dagger)$ , and the total Hamiltonian becomes

$$H_T = H_0 + g_x \sigma_x (b + b^\dagger) + g_z \sigma_z (a + a^\dagger), \quad (3)$$

where  $H_0 = \omega_q/2 \sigma_z + \omega_m b^\dagger b + \omega_c a^\dagger a$ , is the free part with  $\omega_q$ ,  $\omega_m$  and  $\omega_c$  being the qubit, mechanical and optical mode eigenfrequencies, respectively. We interpret  $H_{\text{qc}}$  as the quantized optical field operator  $\zeta = a + a^\dagger$  modulating the qubit frequency as  $\omega_q \rightarrow \omega_q + 2g_z \zeta$ . Assuming that  $\omega_q \gg \omega_m$ , we approximately expand the dispersive interaction Hamiltonian  $H_0^{\text{dis}}$  to second order in  $\xi$  to obtain:

$$H_{\text{int}}(\xi) = \sum_{n=0}^{\infty} G_n \xi^n \sigma_z (b^\dagger + b)^2, \quad (4a)$$

$$G_n = \frac{1}{n!} \frac{\partial^n \chi(\xi)}{\partial \xi^n} \Big|_{\xi=0} \simeq (-1)^n \frac{g_x^2}{\omega_q^{n+1}} (2g_z)^n. \quad (4b)$$

The qubit degree of freedom can be fixed by setting  $\sigma_z = -1$ , since it is practically unexcited. The zero-order

terms only renormalize the mechanical frequency by  $G_0$ . The first-order term in Eq. (S11a) (with strength  $G_1$ ) corresponds to the exact UOM interaction in Eq. (2). The rates of higher-order terms decrease quickly given that  $\omega_q \gg 2g_z\langle\xi\rangle$ , and therefore, can be neglected [38].

Since the mechanical boundary condition is modulated with a fast-oscillating optical field, the quadratic terms  $b^2$  and  $b^{\dagger 2}$  in Eq. (2) cannot be dropped. To obtain an exact analog of  $H'_{\text{COM}}$ , one can employ a low-frequency optical resonator. Consequently, the rapidly oscillating terms, describing two-phonon processes, can be neglected. The UOM interaction can be reduced to

$$H'_{\text{UOM}} = 2G_1 b^\dagger b (a + a^\dagger). \quad (5)$$

An alternative method is to shift the effective optical frequency via a parametric modulation of the longitudinal coupling [39, 40]. Specifically, assuming that  $g_z$  is modulated at a frequency close to  $\omega_c$ , the effective optical frequency  $\omega'_c = (\omega_c - \omega_d)$  is shifted, becoming much smaller than  $\omega_m$ . Therefore, the quadratic terms can also be safely neglected, thus, obtaining Eq. (5). Similar to the mechanism how radiation pressure acts on a macroscopic mirror [29],  $H'_{\text{UOM}}$  describes how *acoustic intensity* (or “phonon pressure”, proportional to  $\langle b^\dagger b \rangle$ ) *induces motions of the optical “position” operator* ( $a + a^\dagger$ ).

*An example of an UOM system.*—Although this method for producing the UOM interactions is very general and can be applied to various types of quantum platforms, we briefly present an UOM example shown in Fig. 1(b), which includes a charge qubit [26] piezoelectrically coupled to a SAW resonator via the qubit capacitances  $C_q$  [41–47]. The qubit frequency is controlled by the static external flux  $\Phi_{\text{ext}}$  through a split-junction loop. A TLR *longitudinally* interacts with the charge qubit via mutual inductance  $M$  [48, 49]. The parametrically modulated longitudinal coupling between the qubit and  $\lambda/4$  (quarter-wavelength) TLR can be realized by applying a time-dependent flux through the qubit loop [38, 39].

The proposed UOM system differs from a COM system as follows: First, *the phonon-resonator boundary condition is modulated via a fast-oscillating optical field*. Therefore, we cannot drop the quadratic term (as we do for a COM system), which can induce observable quantum effects. Second, the COM Hamiltonian results from radiation pressure. However, the UOM interaction is mediated via a qubit, and has no relation to moving the massive phonon mirrors via an optical (microwave) field. Indeed, it originates from a dispersive coupling being modulated by a quantized optical field. Due to these differences, the UOM interaction enables to observe some unconventional quantum phenomena. Below, by considering the SAW-resonator-based UOM system as an example, we show some possible quantum-control applications.

*Modulating the SAW-resonator frequency.*— Using a large mutual inductance, the TLR-qubit interaction strength can easily enter into the strong- or even ultra-strong-coupling regimes [26, 30]. The SAW-qubit coupling reaches tens of MHz in experiments [45, 47]. By setting  $g_x/(2\pi) = 60$  MHz,  $g_z/(2\pi) = 40$  MHz,  $\omega_q/(2\pi) = 3$  GHz, and  $\omega_m/(2\pi) = 250$  MHz, one can obtain a single-phonon UOM coupling strength  $G_1/(2\pi) \simeq -32$  kHz, which is significantly enhanced compared to a direct coupling via the piezoelectric effect. We assume these values in our numerical calculations [50, 51].

Analogously to COM, the optical field operator modifies the mechanical frequency as  $\bar{\omega}_m = [\omega_m^2 - 4G_1\omega_m\langle a^\dagger + a \rangle]^{1/2}$ . To show this, we diagonalize Eq. (3), and plot  $(\bar{\omega}_m - \omega_m)$  versus  $\langle\xi\rangle = \langle a^\dagger + a \rangle$  in Fig. 2(a). Clearly, the effective mechanical frequency is shifted away from  $\omega_m$  by increasing  $\langle\xi\rangle$ . To derive  $H_{\text{UOM}}$  in Eq. (2), we just expand to first order in  $\langle\xi\rangle$ , by assuming  $2g_z\langle\xi\rangle \ll \omega_q$ . Therefore, our analytical formula for the shifted frequency slightly differs from the numerical results when  $\langle\xi\rangle \gg 1$ .

Note that the TLR can be replaced by a 1D microwave guide [26], which allows us to apply a classical microwave field. We assume that the current drive signal is  $I(t) = \Theta(t)I_c$ , where  $\Theta(t)$  is the Heaviside unit step function, and  $I_c$  is the dc current strength applied in the 1D microwave guide when  $t \geq 0$ . The longitudinal coupling is replaced with the classical step drive  $H_\Theta = \Omega_s \sigma_z \Theta(t)$ , which will change the frequency and length of the SAW resonator with amounts  $\delta\omega_m \simeq (4g_x^2\Omega_s)/(\omega_q^2)$  and  $\delta L = (\delta\omega_m L_0)/\omega_m$ , respectively. The whole process is depicted by the green arrow in Fig. 2(a). Therefore, to effectively modify the SAW-resonator resonance frequency, one can simply apply a current bias on the qubit longitudinal degree of freedom.

*Nonlinear transducer, amplifier and Kerr-coupler.*— The phonon-resonator boundary condition in an UOM system is modulated by an optical field at an ultrahigh rate, which can easily exceed the phonon-resonator frequency. By setting  $\omega_c = 2\omega_m$ , one can reduce  $H_{\text{UOM}}$  to a simpler MPA Hamiltonian  $H_{\text{MPA}} = G_1(a^\dagger b^2 + ab^{\dagger 2})$ , which describes the splitting of a photon in the optical cavity into two phonons in the SAW resonator. We denote  $|g(e), n, m\rangle$  for the system containing  $n$  photons and  $m$  phonons, with the qubit in its ground (excited) state. In Fig. 2(b) we plot the third to sixth energy-levels versus the TLR frequency  $\omega_c$ . The anticrossings between the states  $|g, n, m\rangle$  and  $|g, n-1, m+2\rangle$  occur at  $\omega_c = 2\omega_m$ , which result from the nonlinear UOM quadratic coupling.

By assuming that the system is initially in the state  $|g, 1, 0\rangle$ , the quadratic interaction  $H_{\text{MPA}}$  can be verified clearly from Fig. 2(c), which shows the Rabi oscillations between the states  $|g, 0, 2\rangle$  and  $|g, 1, 0\rangle$  (solid curves, governed by the original qubit-intermediated

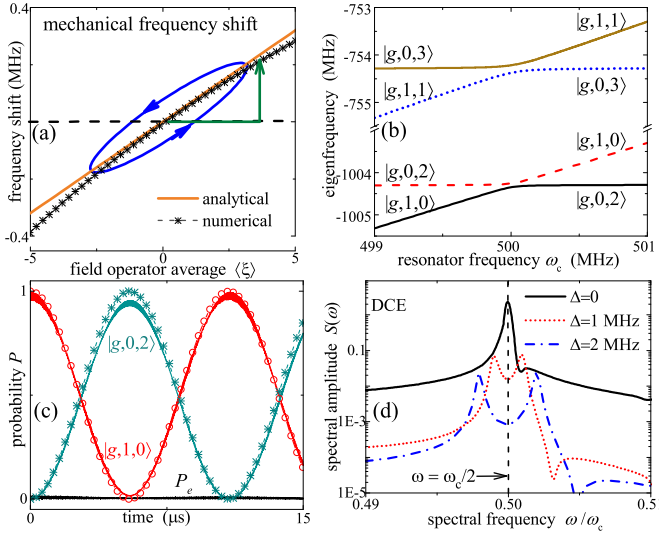


FIG. 2. (a) Mechanical frequency shift ( $\bar{\omega}_m - \omega_m$ ) versus the field operator average  $\langle \xi \rangle = \langle a^\dagger + a \rangle$ . The solid (asterisk) curve corresponds to the analytical (numerical) results. In numerical eigenproblem calculations, the shifted mechanical frequency is defined as the difference between the first and second eigenvalues in the subspace of the qubit ground state  $|g\rangle$ . The mechanical frequency can be suddenly (periodically) modulated via with a step longitudinal bias (an oscillating electromagnetic field) along the green vertical arrow (the blue loop). (b) The third to sixth energy levels of the tripartite system (obtained by diagonalizing  $H_T$ ) versus the SAW frequency  $\omega_c$ . (c) The Rabi oscillations between the states  $|g, 0, 2\rangle$  and  $|g, 1, 0\rangle$ . The solid curves (symbols) represent the evolution described by the original Hamiltonian  $H_T$  (the reduced Hamiltonian  $H_{MPA}$ ).  $P_e$  is the probability of finding the qubit in its excited state. (d) Phonon output spectrum density  $S(\omega)$  for different detuning cases.

Hamiltonian  $H_T$ ). The curves with symbols correspond to  $H_{MPA}$ , which well match the exact results. During this photon-phonon conversion, the qubit-excited probability  $P_e$ , oscillates with an ultralow amplitude above zero (the black curve). Thus, we can safely neglect the qubit degree of freedom when deriving the effective UOM Hamiltonian. This coherent process allows to convert two phonons into one photon, which indicates that the UOM system can serve as a *nonlinear mechanical-optical transducer*. Given that the optical field is strongly driven by a coherent field, we can approximately replace the field operator with a classical amplitude  $\alpha$ , i.e.,  $a \rightarrow \alpha$ . Under this condition, the UOM system can serve as a *mechanical phase-sensitive amplifier*, which can be employed for enhancing ultraweak mechanical quadrature signals for, e.g., quantum detection [52, 53]. Moreover, given that  $\delta_s = \omega_c - 2\omega_m \gg G_1$ , a *phonon-photon cross-Kerr interaction* (Kerr-coupler) can be obtained [38], which can be employed for phonon quantum nondemolition (QND) measurements and phonon distribution counting [54, 55].

Note that  $H_{MPA}$  has the same form as the optomechanical quadratic-interaction in a membrane-in-middle cavity system [27, 56, 57], in which various quantum-control applications, such as mechanical squeezing, photon blockade, and the generation of macroscopically distinct superposition state (Schrödinger cat-like states) [52, 58–62], were proposed. However, few coherent dynamical experiments were successfully demonstrated due to the ultraweak quadratic-coupling strength. The interaction  $H_{MPA}$  can mimic this coupling with a much stronger strength (enhanced by the qubit), and, therefore, provide an effective method to realize these effects.

*Phonon dynamical Casimir effect.*—Analogously to the optical DCE with an optomechanical system, as shown in Fig. 1(b), we consider a modulation of the effective SAW-resonator length  $L$  by a rapidly oscillating optical field [12], and describe the *phonon DCE* based on the UOM system [63, 64].

Since Eq. (2) can be interpreted as quantized photons changing the effective distance  $L_0$  between two phonon mirrors periodically along the blue loop in Fig. 1(a) [3], one can alter the mode intensity of the *acoustic quantum vacuum* by the optical field [12]. In Fig. 2(b), the anticrossing corresponds to the vacuum Casimir-Rabi splitting [14], and we can observe the phonon DCE in an UOM system. In Fig. 2(d), assuming the TLR is resonantly driven with strength  $\epsilon/(2\pi) = 0.05$  MHz, we plot the phonon output spectrum density  $S(\omega)$  for different values of the detuning  $\Delta_d = \omega_c - 2\omega_m$ . When  $\Delta_d = 0$ , the phonon-flux density spectrum shows a single peak at  $\omega = \omega_s/2$ . When  $\Delta_d \neq 0$  [Fig. 2(d)],  $S(\omega)$  shows a symmetric bimodal spectrum at  $\omega'$  and  $\omega''$  with  $\omega' + \omega'' = \omega_c$ , which is a strong indication of the *phonon DCE* where excitations are created in pairs [Fig. 1(b)]. Compared with the resonance case, the emitted phonon pairs are not degenerate any more, but distributed into two conjugate modes with different frequencies [38].

To observe the *optical DCE*: (i) the mechanical mode should oscillate at an ultra-high frequency (corresponding to moving the mirror near the speed of light, instead of the speed of sound for the phonon case), and (ii) a strong optomechanical interaction should be induced [9–12]. Both requirements are exceedingly challenging in experiments. So far, no experiment has successfully demonstrated a real optical DCE involving the mechanical-optical energy conversion [14]. However, the *phonon DCE* described here is much easier to induce and observe, since the boundary condition is modulated by a microwave field: The electromagnetic frequency can easily overwhelm the phonon resonator frequency. Moreover, a strong mechanical-optical UOM coupling, which is enhanced by the intermediate qubit, enables observing the phonon DCE at the quantum level.

*Conclusions.*—We proposed an UOM mechanism, which describes how the frequency of a mechanical mode is effectively modulated by a quantized optical field.



We presented a general method to enhance the UOM coupling via an intermediate qubit. For example, by considering a SAW resonator, we found that the effective resonator length is not fixed, but can be shifted in a large range by simply applying a longitudinal bias on the qubit, which allows more controllability in SAW-resonator experiments. In principle, analogous of various quantum effects studied in COM, can be demonstrated in UOM systems, but with the interchanged roles of photons and phonons. Recently, quantum acoustodynamics has emerged as a powerful platform to explore quantum features of acoustic waves. The UOM mechanism allows to manipulate itinerant phonons at the quantum level [42, 43, 45, 47, 65, 66]. For example, an UOM system can serve as a *nonlinear transducer converting quantum information between acoustic waves and microwave resonators*. Other examples include: mechanical phase-sensitive amplification, cross-Kerr photon-phonon interaction, and phonon DCE. We hope that even other quantum mechanisms and applications can be developed in UOM systems in future studies.

*Acknowledgments.*— The authors acknowledge fruitful discussions with Dr. Anton Frisk Kockum and Sergey Shevchenko. X.W. is supported by the China Postdoctoral Science Foundation No. 2018M631136, and the Natural Science Foundation of China (Grant No. 11804270). A.M. and F.N. acknowledge the support of a grant from the John Templeton Foundation. F.N. is supported in part by the: MURI Center for Dynamic Magneto-Optics via the Air Force Office of Scientific Research (AFOSR) (FA9550-14-1-0040), Army Research Office (ARO) (Grant No. 73315PH), Asian Office of Aerospace Research and Development (AOARD) (Grant No. FA2386-18-1-4045), Japan Science and Technology Agency (JST) (the Q-LEAP program, and CREST Grant No. JPMJCR1676), Japan Society for the Promotion of Science (JSPS) (JSPS-RFBR Grant No. 17-52-50023), and the RIKEN-AIST Challenge Research Fund.

- 
- [1] W. P. Bowen and G. J. Milburn, *Quantum optomechanics* (CRC press, 2015).
  - [2] M. Aspelmeyer, T. J. Kippenberg, and F. Marquardt, *Cavity optomechanics: nano- and micromechanical resonators interacting with light* (Springer, 2014).
  - [3] C. K. Law, “Interaction between a moving mirror and radiation pressure: A Hamiltonian formulation,” *Phys. Rev. A* **51**, 2537 (1995).
  - [4] S. Bose, K. Jacobs, and P. L. Knight, “Preparation of nonclassical states in cavities with a moving mirror,” *Phys. Rev. A* **56**, 4175 (1997).
  - [5] A. Bassi, K. Lochan, S. Satin, T. P. Singh, and H. Ulbricht, “Models of wave-function collapse, underlying theories, and experimental tests,” *Rev. Mod. Phys.* **85**, 471 (2013).
  - [6] M. P. Blencowe, “Effective field theory approach to gravitationally induced decoherence,” *Phys. Rev. Lett.* **111**, 021302 (2013).
  - [7] G. Schaller, R. Schützhold, G. Plunien, and G. Soff, “Dynamical Casimir effect in a leaky cavity at finite temperature,” *Phys. Rev. A* **66**, 023812 (2002).
  - [8] W.-J. Kim, J. H. Brownell, and R. Onofrio, “Detectability of dissipative motion in quantum vacuum via superradiance,” *Phys. Rev. Lett.* **96**, 200402 (2006).
  - [9] J. R. Johansson, G. Johansson, C. M. Wilson, and F. Nori, “Dynamical Casimir effect in a superconducting coplanar waveguide,” *Phys. Rev. Lett.* **103**, 147003 (2009).
  - [10] J. R. Johansson, G. Johansson, C. M. Wilson, and F. Nori, “Dynamical Casimir effect in superconducting microwave circuits,” *Phys. Rev. A* **82**, 052509 (2010).
  - [11] C. M. Wilson, G. Johansson, A. Pourkabirian, M. Simoen, J. R. Johansson, T. Duty, F. Nori, and P. Delsing, “Observation of the dynamical Casimir effect in a superconducting circuit,” *Nature (London)* **479**, 376 (2011).
  - [12] P. D. Nation, J. R. Johansson, M. P. Blencowe, and F. Nori, “Colloquium: Stimulating uncertainty: Amplifying the quantum vacuum with superconducting circuits,” *Rev. Mod. Phys.* **84**, 1 (2012).
  - [13] J. R. Johansson, G. Johansson, C. M. Wilson, P. Delsing, and F. Nori, “Nonclassical microwave radiation from the dynamical Casimir effect,” *Phys. Rev. A* **87**, 043804 (2013).
  - [14] V. Macrì, A. Ridolfo, O. Di Stefano, A. F. Kockum, F. Nori, and S. Savasta, “Nonperturbative dynamical Casimir effect in optomechanical systems: Vacuum Casimir-Rabi splittings,” *Phys. Rev. X* **8**, 011031 (2018).
  - [15] O. Di Stefano, A. Settineri, V. Macrì, A. Ridolfo, R. Stassi, A. F. Kockum, S. Savasta, and F. Nori, “Interaction of mechanical oscillators mediated by the exchange of virtual photon pairs,” *Phys. Rev. Lett.* **122**, 030002 (2019).
  - [16] W. Marshall, C. Simon, R. Penrose, and D. Bouwmeester, “Towards quantum superpositions of a mirror,” *Phys. Rev. Lett.* **91**, 130401 (2003).
  - [17] J.-Q. Liao and L. Tian, “Macroscopic quantum superposition in cavity optomechanics,” *Phys. Rev. Lett.* **116**, 163602 (2016).
  - [18] I. Carusotto, R. Balbinot, A. Fabbri, and A. Recati, “Density correlations and analog dynamical Casimir emission of Bogoliubov phonons in modulated atomic Bose-Einstein condensates,” *Eur. Phys. J. D* **56**, 391 (2009).
  - [19] D. Boiron, A. Fabbri, P.-É. Larré, N. Pavloff, C. I. Westbrook, and P. Ziñ, “Quantum signature of analog Hawking radiation in momentum space,” *Phys. Rev. Lett.* **115**, 025301 (2015).
  - [20] S. Eckel, A. Kumar, T. Jacobson, I. B. Spielman, and G. K. Campbell, “A rapidly expanding Bose-Einstein condensate: An expanding universe in the lab,” *Phys. Rev. X* **8**, 021021 (2018).
  - [21] B. G. Taketani, R. P. Schmit and F. K. Wilhelm, “Quantum simulation of Hawking radiation with surface acoustic waves,” *preprint arXiv:1804.04092* (2018).
  - [22] D. Rugar and P. Grütter, “Mechanical parametric amplification and thermomechanical noise squeezing,” *Phys. Rev. Lett.* **67**, 699 (1991).
  - [23] D. W. Carr, S. Evoy, L. Sekaric, H. G. Craighead, and

- J. M. Parpia, “Parametric amplification in a torsional microresonator,” *Appl. Phys. Lett.* **77**, 1545 (2000).
- [24] M. Zalalutdinov, A. Olkhovets, A. Zehnder, B. Ilic, D. Czaplewski, H. G. Craighead, and J. M. Parpia, “Optically pumped parametric amplification for micromechanical oscillators,” *Appl. Phys. Lett.* **78**, 3142 (2001).
- [25] R. B. Karabalin, S. C. Masmanidis, and M. L. Roukes, “Efficient parametric amplification in high and very high frequency piezoelectric nanoelectromechanical systems,” *Appl. Phys. Lett.* **97**, 183101 (2010).
- [26] X. Gu, A. F. Kockum, A. Miranowicz, Y.-X. Liu, and F. Nori, “Microwave photonics with superconducting quantum circuits,” *Phys. Rep.* **718-719**, 1 (2017).
- [27] J. D. Thompson, B. M. Zwickl, A. M. Jayich, F. Marquardt, S. M. Girvin, and J. G. E. Harris, “Strong dispersive coupling of a high-finesse cavity to a micromechanical membrane,” *Nature (London)* **452**, 72 (2008).
- [28] D. E. Bruschi and A. Xuereb, “Mechano-optics: an optomechanical quantum simulator,” *New J. of Phys.* **20**, 065004 (2018).
- [29] M. Aspelmeyer, T. J. Kippenberg, and F. Marquardt, “Cavity optomechanics,” *Rev. Mod. Phys.* **86**, 1391 (2014).
- [30] A. F. Kockum, A. Miranowicz, S. De Liberato, S. Savasta, and F. Nori, “Ultrastrong coupling between light and matter,” *Nature Reviews Physics* **1**, 19–40 (2019).
- [31] T. T. Heikkilä, F. Massel, J. Tuorila, R. Khan, and M. A. Sillanpää, “Enhancing optomechanical coupling via the Josephson effect,” *Phys. Rev. Lett.* **112**, 203603 (2014).
- [32] J.-M. Pirkkalainen, S.U. Cho, F. Massel, J. Tuorila, T.T. Heikkilä, P.J. Hakonen, and M.A. Sillanpää, “Cavity optomechanics mediated by a quantum two-level system,” *Nat. Commun.* **6**, 6981 (2015).
- [33] D. Zueco, G. M. Reuther, S. Kohler, and P. Hänggi, “Qubit-oscillator dynamics in the dispersive regime: Analytical theory beyond the rotating-wave approximation,” *Phys. Rev. A* **80**, 033846 (2009).
- [34] Y. J. Zhao, Y. L. Liu, Y. X. Liu, and F. Nori, “Generating nonclassical photon states via longitudinal couplings between superconducting qubits and microwave fields,” *Phys. Rev. A* **91**, 053820 (2015).
- [35] X. Wang, A. Miranowicz, H.-R. Li, and F. Nori, “Observing pure effects of counter-rotating terms without ultrastrong coupling: A single photon can simultaneously excite two qubits,” *Phys. Rev. A* **96**, 063820 (2017).
- [36] R. Stassi and F. Nori, “Long-lasting quantum memories: Extending the coherence time of superconducting artificial atoms in the ultrastrong-coupling regime,” *Phys. Rev. A* **97**, 033823 (2018).
- [37] N. Lambert, M. Cirio, M. Delbecq, G. Allison, M. Marx, S. Tarucha, and F. Nori, “Amplified and tunable transverse and longitudinal spin-photon coupling in hybrid circuit-QED,” *Phys. Rev. B* **97**, 125429 (2018).
- [38] See Supplementary Material at <http://xxx> for detailed derivations of our main results, also citing [67–73].
- [39] N. Didier, J. Bourassa, and A. Blais, “Fast quantum nondemolition readout by parametric modulation of longitudinal qubit-oscillator interaction,” *Phys. Rev. Lett.* **115**, 203601 (2015).
- [40] M. Cirio, K. Debnath, N. Lambert, and F. Nori, “Amplified optomechanical transduction of virtual radiation pressure,” *Phys. Rev. Lett.* **119**, 053601 (2017).
- [41] M. V. Gustafsson, T. Aref, A. F. Kockum, M. K. Ekström, G. Johansson, and P. Delsing, “Propagating phonons coupled to an artificial atom,” *Science* **346**, 207 (2014).
- [42] M. J. A. Schuetz, E. M. Kessler, G. Giedke, L. M. K. Vandersypen, M. D. Lukin, and J. I. Cirac, “Universal quantum transducers based on surface acoustic waves,” *Phys. Rev. X* **5**, 031031 (2015).
- [43] R. Manenti, M. J. Peterer, A. Nersisyan, E. B. Magnusson, A. Patterson, and P. J. Leek, “Surface acoustic wave resonators in the quantum regime,” *Phys. Rev. B* **93**, 041411 (2016).
- [44] T. Aref, P. Delsing, M. K. Ekström, A. F. Kockum, M. V. Gustafsson, G. Johansson, P. J. Leek, E. Magnusson, and R. Manenti, “Quantum acoustics with surface acoustic waves,” in *Quantum Science and Technology* (Springer International Publishing, 2016) p. 217.
- [45] R. Manenti, A. F. Kockum, A. Patterson, T. Behrle, J. Rahamim, G. Tancredi, F. Nori, and P. J. Leek, “Circuit quantum acoustodynamics with surface acoustic waves,” *Nat. Commun.* **8** (2017).
- [46] B. A. Moores, Lucas R. Sletten, J. J. Viennot, and K. W. Lehnert, “Cavity quantum acoustic device in the multimode strong coupling regime,” *Phys. Rev. Lett.* **120**, 227701 (2018).
- [47] A. N. Bolgar, J. I. Zotova, D. D. Kirichenko, I. S. Besedin, A. V. Semenov, R. S. Shaikhaidarov, and O. V. Astafiev, “Quantum regime of a two-dimensional phonon cavity,” *Phys. Rev. Lett.* **120**, 223603 (2018).
- [48] E. Sánchez-Burillo, L. Martín-Moreno, J. J. García-Ripoll, and D. Zueco, “Full two-photon down-conversion of a single photon,” *Phys. Rev. A* **94**, 053814 (2016).
- [49] X. Li, Y. Ma, J. Han, T. Chen, Y. Xu, W. Cai, H. Wang, Y.P. Song, Z.-Y. Xue, Z.-Q. Yin, and L.-Y. Sun, “Perfect quantum state transfer in a superconducting qubit chain with parametrically tunable couplings,” *Phys. Rev. Applied* **10**, 054009 (2018).
- [50] J. R. Johansson, P. D. Nation, and F. Nori, “Qutip 2: A Python framework for the dynamics of open quantum systems,” *Comput. Phys. Commun.* **184**, 1234 (2013).
- [51] J. R. Johansson, P. D. Nation, and F. Nori, “Qutip: An open-source Python framework for the dynamics of open quantum systems,” *Comput. Phys. Commun.* **183**, 1760 (2012).
- [52] A. Nunnenkamp, K. Børkje, J. G. E. Harris, and S. M. Girvin, “Cooling and squeezing via quadratic optomechanical coupling,” *Phys. Rev. A* **82**, 021806 (2010).
- [53] A. A. Clerk, M. H. Devoret, S. M. Girvin, Florian Marquardt, and R. J. Schoelkopf, “Introduction to quantum noise, measurement, and amplification,” *Rev. Mod. Phys.* **82**, 1155 (2010).
- [54] W. J. Munro, K. Nemoto, R. G. Beausoleil, and T. P. Spiller, “High-efficiency quantum-nondemolition single-photon-number-resolving detector,” *Phys. Rev. A* **71**, 033819 (2005).
- [55] S.-Q. Ding, G. Maslennikov, R. Hablützel, and D. Matsukevich, “Cross-Kerr nonlinearity for phonon counting,” *Phys. Rev. Lett.* **119**, 193602 (2017).
- [56] J. C. Sankey, C. Yang, B. M. Zwickl, A. M. Jayich, and J. G. E. Harris, “Strong and tunable nonlinear optomechanical coupling in a low-loss system,” *Nat.*

- Phys. **6**, 707 (2010).
- [57] J.-Q. Liao and F. Nori, “Single-photon quadratic optomechanics,” *Sci. Rep.* **4**, 6302 (2014).
  - [58] H.-T. Tan, F. Bariani, G.-X. Li, and P. Meystre, “Generation of macroscopic quantum superpositions of optomechanical oscillators by dissipation,” *Phys. Rev. A* **88**, 023817 (2013).
  - [59] J.-Q. Liao and F. Nori, “Photon blockade in quadratically coupled optomechanical systems,” *Phys. Rev. A* **88**, 023853 (2013).
  - [60] E.-J. Kim, J. R. Johansson, and F. Nori, “Circuit analog of quadratic optomechanics,” *Phys. Rev. A* **91**, 033835 (2015).
  - [61] X. Wang, A. Miranowicz, H.-R. Li, and F. Nori, “Hybrid quantum device with a carbon nanotube and a flux qubit for dissipative quantum engineering,” *Phys. Rev. B* **95**, 205415 (2017).
  - [62] C. S. Muñoz, A. Lara, J. Puebla, and F. Nori, “Hybrid systems for the generation of nonclassical mechanical states via quadratic interactions,” *Phys. Rev. Lett.* **121**, 123604 (2018).
  - [63] J.-C. Jaskula, G. B. Partridge, M. Bonneau, R. Lopes, J. Ruaudel, D. Boiron, and C. I. Westbrook, “Acoustic analog to the dynamical Casimir effect in a Bose-Einstein condensate,” *Phys. Rev. Lett.* **109**, 220401 (2012).
  - [64] A. Motazedifard, M. H. Naderi, and R. Roknizadeh, “Dynamical Casimir effect of phonon excitation in the dispersive regime of cavity optomechanics,” *J. Opt. Soc. Am. B* **34**, 642 (2017).
  - [65] P. Delsing, A. F. Kockum and G. Johansson, “Designing frequency-dependent relaxation rates and lamb shifts for a giant artificial atom,” *Phys. Rev. A* **90**, 013837 (2014).
  - [66] A. F. Kockum, G. Johansson, and F. Nori, “Decoherence-free interaction between giant atoms in waveguide quantum electrodynamics,” *Phys. Rev. Lett.* **120**, 140404 (2018).
  - [67] Y.-X. Liu, C.-X. Yang, H.-C. Sun, and X.-B. Wang, “Coexistence of single- and multi-photon processes due to longitudinal couplings between superconducting flux qubits and external fields,” *New J. Phys.* **16**, 015031 (2014).
  - [68] S. Richer, N. Maleeva, S. T. Skacel, I. M. Pop, and D. DiVincenzo, “Inductively shunted transmon qubit with tunable transverse and longitudinal coupling,” *Phys. Rev. B* **96**, 174520 (2017).
  - [69] E. A. Sete, J. M. Martinis, and A. N. Korotkov, “Quantum theory of a bandpass purcell filter for qubit readout,” *Phys. Rev. A* **92**, 012325 (2015).
  - [70] J. J. Viennot, X. Ma, and K. W. Lehnert, “Phonon-number-sensitive electromechanics,” *Phys. Rev. Lett.* **121**, 183601 (2018).
  - [71] M. O. Scully and M. S. Zubairy, *Quantum Optics* (Cambridge University Press, Cambridge, 1997).
  - [72] P. Lähteenmäki, G. S. Paraoanu, J. Hassel, and P. J. Hakonen, “Dynamical Casimir effect in a Josephson metamaterial,” *PNAS* **110**, 4234 (2013).
  - [73] A. Lambrecht, M. Jaekel, and S. Reynaud, “Motion induced radiation from a vibrating cavity,” *Phys. Rev. Lett.* **77**, 615 (1996).

# Supplementary Material for Unconventional Cavity Optomechanics: Nonlinear Control of Phonons in the Acoustic Quantum Vacuum

Xin Wang<sup>1,2</sup>, Wei Qin<sup>2</sup>, Adam Miranowicz<sup>2,3</sup>, Salvatore Savasta<sup>2,4</sup> and Franco Nori<sup>2,5</sup>

<sup>1</sup>*Institute of Quantum Optics and Quantum Information, School of Science, Xi'an Jiaotong University, Xi'an 710049, China*

<sup>2</sup>*Theoretical Quantum Physics Laboratory, RIKEN Cluster for Pioneering Research, Wako-shi, Saitama 351-0198, Japan,*

<sup>3</sup>*Faculty of Physics, Adam Mickiewicz University, 61-614 Poznań, Poland*

<sup>4</sup>*Dipartimento di Scienze Matematiche e Informatiche, Scienze Fisiche e Scienze della Terra, Università di Messina, I-98166 Messina, Italy*

<sup>5</sup>*Physics Department, The University of Michigan, Ann Arbor, Michigan 48109-1040, USA*

This supplementary material includes: In Sec. I, detailed derivations of unconventional cavity optomechanics (UOM) mediated by a qubit. In Sec. II, a possible proposal to realize the UOM interaction based on superconducting quantum circuits coupled to a surface acoustic resonator. In Sec. III, a proposal on how to observe phonon dynamical Casimir effect in an UOM system.

## S1. UNCONVENTIONAL OPTOMECHANICAL HAMILTONIAN

We now present detailed derivations of unconventional cavity optomechanics (UOM) mediated by a qubit. We start our discussions by first considering a mechanical oscillator interacting with a qubit with strength  $g_x$ , i.e.,

$$H_{\text{qm}} = \frac{1}{2}\omega_q\sigma_z + \omega_m b^\dagger b + g_x\sigma_x(b^\dagger + b), \quad (\text{S1})$$

where  $b$  ( $b^\dagger$ ) are the annihilation (creation) operators of the mechanical mode,  $\omega_q$  is the qubit transition frequency, while  $\sigma_z = |e\rangle\langle e| - |g\rangle\langle g|$  and  $\sigma_x = |e\rangle\langle g| + |g\rangle\langle e|$  are the qubit Pauli operators with  $|e\rangle$  ( $|g\rangle$ ) being the excited (ground) state. We assume that the system is largely detuned with  $(\omega_q - \omega_m) \gg g_x$ . The optical cavity is involved in this bipartite system by considering its longitudinal coupling with the qubit [S1–S4], which is described by the Hamiltonian

$$H_{\text{qc}} = g_{z0} \cos(\omega_d t) \sigma_z (a^\dagger + a), \quad (\text{S2})$$

where  $a$  ( $a^\dagger$ ) are the annihilation (creation) operators of the optical mode. As in Ref. [S5], we consider a general case, where the *longitudinal coupling*  $g_{z0}$  is *parametrically modulated* at a frequency  $\omega_d$ . Note that the following discussions can also be applied to the constant longitudinal case. Consequently, the system Hamiltonian becomes

$$H_0 = \frac{1}{2}\omega_q\sigma_z + \omega_{c0}a^\dagger a + \omega_m b^\dagger b + g_{z0} \cos(\omega_d t) \sigma_z (a^\dagger + a) + g_x\sigma_x(b^\dagger + b), \quad (\text{S3})$$

where  $\omega_{c0}$  is the resonator frequency. By rotating the resonator at frequency  $\omega_d$ , and neglecting the rapidly oscillating terms, we obtain

$$H_1 = \frac{\omega_q}{2}\sigma_z + \omega_c a^\dagger a + \omega_m b^\dagger b + g_z \sigma_z (a^\dagger + a) + g_x\sigma_x(b^\dagger + b), \quad (\text{S4})$$

where  $\omega_c = \omega_{c0} - \omega_d$  is the shifted resonator frequency, and  $g_z = g_{z0}/2$  is an effective longitudinal coupling strength. Later we find that this modulation allows us to obtain an exact analogue of the conventional optomechanical Hamiltonian by dropping the quadratic terms.

By setting  $\xi = (a^\dagger + a)$ , the longitudinal interaction can be viewed as the quantized optical field modulating the qubit transition frequency as  $\omega_q(\xi) = \omega_q + 2g_z\xi$ . Here we assume that the qubit-mechanical interaction is in the dispersive regime. By defining  $X_\pm = \sigma_- b^\dagger \pm \sigma_+ b$  and  $Y_\pm = \sigma_+ b^\dagger \pm \sigma_- b$ , we can rewrite  $H_1$  as

$$H_2 = \frac{1}{2}\omega_q(\xi)\sigma_z + \omega_c a^\dagger a + \omega_m b^\dagger b + g_x (X_+ + Y_+). \quad (\text{S5})$$



Different from the standard derivations of dispersive coupling under the rotating wave approximation, we also consider the counter-rotating term  $Y_+$  in  $H_2$ . Applying the unitary transformation [S6],

$$U = \exp [\lambda_-(\xi)X_- + \lambda_+(\xi)Y_-], \quad \lambda_{\pm}(\xi) = \frac{g_x}{\omega_q(\xi) \pm \omega_c}, \quad (\text{S6})$$

to  $H_2$ , we can expand the transformed Hamiltonian  $\tilde{H} = U^\dagger H_2 U$  to first order in the small parameters  $\lambda_{\pm}(\xi)$ . Thus, we obtain the following dispersive-type coupling Hamiltonian

$$\tilde{H} \simeq H_0 + H_{\text{int}}, \quad (\text{S7})$$

$$H_0(\xi) = \frac{\omega_q(\xi)}{2} \sigma_z + \omega_c a^\dagger a + \omega_m b^\dagger b, \quad (\text{S8})$$

$$H_{\text{int}}(\xi) = \frac{1}{2} \sigma_z g_x [\lambda_+(\xi) + \lambda_-(\xi)] (b^\dagger + b)^2. \quad (\text{S9})$$

Comparing with the standard dispersive coupling, we find two differences in Eq. (S9): First, due to counter-rotating contributions, the quadratic terms  $b^2$  and  $b^{\dagger 2}$  are also involved. Second, more importantly, the dispersive coupling strength,

$$\chi(\xi) = \frac{1}{2} g_x [\lambda_+(\xi) + \lambda_-(\xi)] = \frac{g_x^2 \omega_q(\xi)}{\omega_q^2(\xi) - \omega_m^2}, \quad (\text{S10})$$

is not constant but depends on the quantized optical field operator  $\xi = a + a^\dagger$ . Assuming that  $\omega_q \gg 2g_z \xi$  and  $\omega_q \gg \omega_m$ , we approximately expand  $H_{\text{int}}(\xi)$  to second order in  $\xi$ , to obtain:

$$H_{\text{int}}(\xi) = \sum_{n=0}^2 G_n \xi^n \sigma_z (b^\dagger + b)^2 + o(\xi^2), \quad (\text{S11a})$$

$$G_n = \frac{1}{n!} \left. \frac{\partial^n \chi(\xi)}{\partial \xi^n} \right|_{\xi=0} \simeq (-1)^n \frac{g_x^2}{\omega_q^{n+1}} (2g_z)^n. \quad (\text{S11b})$$

We assume that the qubit is initially in its ground state  $|g\rangle$ . Since the qubit is largely detuned from the mechanical mode, phonons cannot effectively excite the qubit. Moreover, the longitudinal coupling commutes with the qubit operator  $\sigma_z$ , which does not cause any qubit state transition either. Therefore, it is reasonable to assume that the qubit is approximately in its ground state with  $\langle \sigma_z \rangle \simeq -1$  in Eq. (S11a). Under these conditions, the zeroth-order term can be reduced to

$$H_{\text{int},0} = G_0 \sigma_z (b^\dagger + b)^2 \simeq -2G_0 b^\dagger b, \quad (\text{S12})$$

which shows that the mechanical frequency is renormalized as  $\omega_m \rightarrow (\omega_m - 2G_0)$ . Moreover, the longitudinal coupling term in Eq. (S8) is reduced as  $-g_z(a + a^\dagger)$ , which results in displacing the optical operator as  $a \rightarrow (a - g_z/\omega_c)$ , and can be eliminated under the condition  $g_z \ll \omega_c$ . The first- and second-order terms in Eq. (S11a) describe the interaction between the mechanical oscillator and the optical field. The corresponding coupling ratio,

$$\left| \frac{G_2}{G_1} \right| = \frac{2g_z}{\omega_q} \ll 1, \quad (\text{S13})$$

is a small parameter. Therefore, we just consider only the first-order term. Since the qubit degree of freedom is effectively eliminated, the Hamiltonian for the mechanical and optical modes can be written as

$$H_s \simeq \omega_c a^\dagger a + \omega_m b^\dagger b - G_1 (b^\dagger + b)^2 (a^\dagger + a). \quad (\text{S14})$$

Given that  $\delta_s = (\omega_c - 2\omega_m) \gg G_1$ , the Hamiltonian reads

$$H_\delta = G_1 [a^\dagger b^2 \exp(i\delta_s t) + ab^{\dagger 2} \exp(-i\delta_s t)],$$

from which we can obtain the cross-Kerr interaction between these two modes [S7], i.e.,

$$H_{\text{ck}} = \frac{2G_1^2}{\delta_s} [a^\dagger a (2b^\dagger b + 1) - b^{\dagger 2} b^2]. \quad (\text{S15})$$

This interaction describes that the average phonon number operator  $\langle n \rangle = \langle b^\dagger b \rangle$ , will effectively shift the optical frequency. Equation. (S11a) also contains a cross-Kerr coupling with strength  $-2G_2$  (a second-order term). Therefore, the phonon number  $\langle n \rangle = \langle b^\dagger b \rangle$  eventually shifts the optical frequency by the amount

$$\delta\omega_c = \chi_k \langle n \rangle, \quad \chi_k = \left[ \frac{4G_1^2}{\delta_s} - 2G_2 \right]. \quad (\text{S16})$$

By setting  $\delta_s = 20G_1$  and adopting the parameters specified in the main article, the optical frequency shift per phonon is about  $\chi_k/(2\pi) \simeq -10$  kHz. Since  $H_{\text{ck}}$  commutes with the phonon-number operator, this interaction can be employed for phonon quantum nondemolition (QND) measurements and phonon distribution counting [S7, S8].

Finally, we discuss the parameter regimes where this qubit-mediated coupling for unconventional cavity optomechanics (UOM) is valid. First, we recall that the effective interaction is based on the dispersive coupling between the mechanical mode and the qubit, which sets a limitation on the average phonon number as  $\langle n \rangle = \langle b^\dagger b \rangle \leq (4\lambda_-)^{-2}$  [S9]. Second, the convergence of the expansion, given in Eq. (S11b), requires that  $\langle \xi \rangle \leq 2g_z/\omega_q$ , which also sets a bound for the optical intracavity field amplitude.

## S2. UNCONVENTIONAL OPTOMECHANICS WITH HYBRID SUPERCONDUCTING CIRCUITS

In the previous section, we showed how to obtain the UOM interaction by employing an intermediate qubit. Although such a method is very general and not specified to any certain quantum platform, we now give an example of UOM systems with a surface acoustic wave (SAW) resonator.

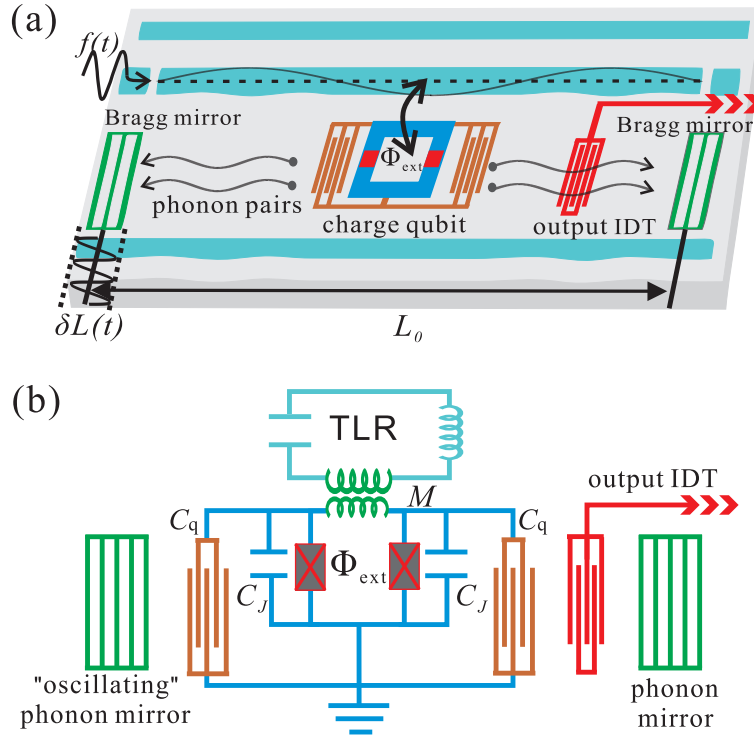


FIG. S1. (a) Schematic diagram and (b) lumped-circuit layout describing an inverse optomechanical (UOM) system based on a surface-acoustic-wave (SAW) resonator: A charge-qubit, with two split Josephson junctions (red bars) is placed into the SAW resonator (confined by two Bragg mirrors). The TLR can be viewed as an LC resonator in the (b). Their interaction is mediated via two identical inter-digitated-transducers (IDTs) of capacitance  $C_q$  via the piezoelectric effects. A transmission-line resonator (TLR) longitudinally couples to the charge-qubit via the mutual inductance  $M$ . The field current operator  $\hat{I}(t)$  effectively changes the SAW resonator length  $L$  by amount  $\delta L(t)$ . One Bragg mirror acts as a fast “oscillating” mirror.

As shown in Fig. S1(a), phonons can be itinerant in a SAW resonator confined by two Bragg phonon mirrors [S10–S14]. Similar to an optical cavity, the  $N$ th resonance acoustic mode depends on the phonon-mirror distance  $L_0$  via the relation,  $\omega_m/(2\pi) = Nv_e/(2L_0)$ , where  $v_e$  is the sound speed along the crystal surface. Here we consider

a charge qubit [S9] with two symmetric Josephson junctions (with Josephson energy  $E_J$ ) placed inside the phonon resonator. The two junctions of the charge qubit form a superconducting quantum interference device (SQUID), and the total Josephson energy can be controlled via the external flux  $\Phi_{\text{ext}}$  through it. The qubit capacitance  $C_q$  of an interdigitated-transducer (IDT) type shares the same periodicity with the resonator acoustic mode. The Hamiltonian for the charge qubit can be expressed as [S9]:

$$H_q = 4E_C(\hat{n} - n_g)^2 - 2E_J \cos\left(\frac{\pi\Phi_{\text{ext}}}{\Phi_0}\right) \cos\phi, \quad (\text{S17})$$

where  $E_C = e^2/(2C_\Sigma)$  is the total charging energy of the two junctions, and  $C_\Sigma = C_J + C_g$  with  $C_J$  being the Josephson capacitance. To suppress the charge noise, one can apply a dc voltage to bias at the charge degeneracy point  $n_g = 1/2$ . The charge qubit Hamiltonian takes the form [S9, S15]:

$$H_q \simeq -4E_C\delta n_g(|1\rangle\langle 1| - |0\rangle\langle 0|) - E_J \cos\left(\frac{\pi\Phi_{\text{ext}}}{\Phi_0}\right) (|1\rangle\langle 0| + |0\rangle\langle 1|), \quad (\text{S18})$$

where  $|0\rangle$  and  $|1\rangle$  are the charge qubit states, and  $\delta n_g = C_q V(t)/(2e)$  is the offset charge deviation from the optimal point, with  $V(t)$  being the external quantized voltage drive. The qubit capacitance  $C_q$  serves as a coupling element between the SAW resonator and the charge qubit. The interaction mechanism can be understood as follows: An acoustic wave travels on the crystal surface, and generates an oscillating voltage  $V(t)$  on the qubit capacitance  $C_q$  due to the piezoelectric effect [S12]. Note that  $V(t)$  is induced by the quantized motion and can be viewed as a time-dependent drive on the charge qubit. Although many discrete acoustic modes can, in principle, be excited in the phonon resonator, only one central mode is strongly coupled to the qubit [S12]. Thus, it is physically justified to consider a single acoustic mode here. The voltage difference is associated with the zero-point mechanical fluctuation  $u_0$  as  $V(t) = u_0(b + b^\dagger)$ . In the rotated basis with  $|e\rangle = (|1\rangle - |0\rangle)/\sqrt{2}$  and  $|g\rangle = (|1\rangle + |0\rangle)/\sqrt{2}$ , the SAW-qubit coupling can be approximately written as [S12]:

$$H_{\text{qm}} = -4E_C\delta n_g\sigma_x = -\frac{eC_q}{C_\Sigma}u_0(b + b^\dagger)\sigma_x, \quad (\text{S19})$$

which corresponds to the transverse coupling between the SAW resonator and the charge qubit.

As depicted in Fig. S1(b), the effective Josephson energy depends on the external flux bias  $\Phi_{\text{ext}}$ . One can couple the charge qubit with a TLR via a mutual inductance  $M$ . The central conductor of the TLR is along the  $x$  direction, and the interaction position is assumed to be at an anti-node point of the current field  $\hat{I}(x, t)$ . The quantized current  $\hat{I} = I_0(a + a^\dagger)$  creates a flux perturbation  $\delta\Phi_{\text{ext}} = MI_0(a + a^\dagger)$  on the qubit static bias flux  $\Phi_{\text{ext}}^0$ , where  $I_0$  is the current zero-point-fluctuation amplitude, and  $a$  ( $a^\dagger$ ) is the annihilation (creation) operator of the microwave photons. Therefore, we can expand the Josephson term in Eq. (S18), to first order in  $\delta\Phi_{\text{ext}}$ , and obtain [S16]:

$$H_q = \frac{\omega_q}{2}\sigma_z + \frac{1}{2}\left(\frac{\partial\omega_q}{\partial\Phi_{\text{ext}}}\right)\Big|_{\Phi_{\text{ext}}^0}\sigma_z\delta\Phi_{\text{ext}}, \quad (\text{S20})$$

$$\omega_q = 2E_J \cos\left(\frac{\pi\Phi_{\text{ext}}}{\Phi_0}\right). \quad (\text{S21})$$

Note that the second term in Eq. (S20) describes the interaction between the charge qubit and the TLR, and can be written as

$$H_{\text{qc}} = g_z(a + a^\dagger)\sigma_z, \quad (\text{S22})$$

where the longitudinal coupling strength is

$$g_z = -\frac{\pi E_J}{\Phi_0} \sin\left(\frac{\pi\Phi_{\text{ext}}}{\Phi_0}\right) MI_0. \quad (\text{S23})$$

Up to now, we considered  $g_z$  to be a constant. A *parametrically modulated longitudinal coupling* between a superconducting qubit and a  $\lambda/4$  (quarter wavelength) TLR can be realized by applying a time-dependent flux through the SQUID loop. A detailed description of the method can be found in Ref. [S5].

In Refs. [S12, S13], the SAW resonator is assumed to couple with a transmon, and their coupling shares a similar expression as in Eq. (S19) for the SAW-qubit coupling, except for a dimensionless parameter. The UOM interaction

mediated by a transmon can also be produced. However, different from the charge qubit, a transmon is a weakly anharmonic system, and the UOM interaction based on a dispersive coupling (as described in Sec. II) will be disturbed by an imperfect state truncation at the first-excited level [S17, S18]. The UOM interaction in Eq. (S11a) should be derived by considering higher-energy levels.

Note that the TLR can be replaced by a 1D microwave guide [S9], to which a classical microwave field can be applied. We assume that the current drive signal is  $I(t) = \Theta(t)I_c$ , where  $\Theta(t)$  is the Heaviside unit step function, and  $I_c$  is the dc current strength applied to the 1D microwave guide when  $t \geq 0$ . The longitudinal coupling should be replaced with the classical step drive  $H_\Theta = \Omega_s \sigma_z \Theta(t)$ , where

$$\Omega_s = -\frac{\pi E_J}{\Phi_0} \sin\left(\frac{\pi \Phi_{\text{ext}}}{\Phi_0}\right) M I_c. \quad (\text{S24})$$

Following the derivations in Sec. I and the discussions in Ref. [S19], the interaction form corresponds to *changing the frequency and the length of the SAW resonator* at  $t = 0$  with amounts

$$\delta\omega_m = \frac{4g_x^2}{\omega_q^2} \Omega_s, \quad \delta L = \frac{\delta\omega_m}{\omega_m} L_0, \quad (\text{S25})$$

respectively. Therefore, to effectively modify the resonance frequency of the SAW resonator, one can simply apply a current bias on the qubit longitudinal degree of freedom.

In addition to the SAW resonator, phonons can also exist in a localized mechanical oscillator. As discussed in Ref. [S20], the transverse-coupling strength between a drum-type mechanical oscillator and a charge qubit can be engineered in the strong-coupling regime (about tens of MHz). By coupling the TLR (or  $LC$ -resonator) quantized electromagnetic field with the split-junction loop of the charge qubit, the required longitudinal interaction can also be induced [S16]. Therefore, one can realize the required Hamiltonian Eq. (S4), to generate the qubit-mediated UOM interaction [Eq. (S14)] for both SAW resonator and localized mechanical resonator.

### S3. PHONON DYNAMICAL CASIMIR EFFECT

As shown in Fig. S1(b), the interaction given by Eq. (S14) can be interpreted as quantized photons changing the effective distance  $L_0$  between two phonon mirrors [S19]. This indicates that the electromagnetic field can alter the mode intensity of the *phonon* field. In Fig. 2(b) of the main article, the anticrossing corresponds to the vacuum Casimir-Rabi splitting [S21]. Analogously to the photon dynamical Casimir effect (DCE) [S22–S24], phonon pairs are emitted due to the modulated-boundary condition of the *acoustic quantum vacuum*.

To verify this, we assume that the intracavity phonons can escape from the SAW resonator from an output channel. As shown in Fig. S1(b), one can employ an interdigitated-transducer (IDT) to convert output phonons into electromagnetic signals (phonons) [S12]. The boundary condition for the output field  $c(t)$  and the intracavity SAW field  $b(t)$  is

$$c(t) = \sqrt{\kappa} b_{\text{in}}(t) + b(t),$$

where  $\kappa$  is the phonon escape rate from the SAW resonator, and  $b_{\text{in}}(t)$  is assumed to be the vacuum input field. The output-phonon number per second is expressed as  $P_{\text{out}} = \kappa \langle c^\dagger c \rangle$ . To describe the correlations between phonons, we define the second-order correlation function as

$$g_2(\tau) = \lim_{t \rightarrow \infty} \frac{\langle c^\dagger(t) c^\dagger(t+\tau) c(t+\tau) c(t) \rangle}{\langle c^\dagger(t) c(t) \rangle^2}$$

with  $\tau$  being the delay time. The phonon-flux spectrum density (detected by IDTs) is defined as

$$S(\omega) = \text{Re} \int_0^\infty \langle c^\dagger(0) c(\tau) \rangle e^{i\omega\tau} d\tau \quad (\text{S26})$$

We note that a phonon power spectrum can also be measured via electromotive techniques (see, e.g., Ref. [S25] and reference therein). According to the Wiener-Khinchin theorem [S26], and by replacing the output operator with the intracavity field, one can find that

$$S(\omega) \propto n_{\text{out}}(\omega) = \int_0^\infty \text{Tr}[\rho b^\dagger(\omega) b(\omega')] d\omega', \quad (\text{S27})$$



where

$$b(\omega) = \frac{1}{\sqrt{2\pi}} \int_{-\infty}^{\infty} b(t) e^{-i\omega t} dt$$

is the Fourier transform of the intracavity field operator  $b(t)$ , and satisfies the canonical commutation relation  $[b(\omega), b^\dagger(\omega')] = \delta(\omega - \omega')$ .

Assuming that the TLR is resonantly driven via a coherent field with strength  $\epsilon$ , i.e.,  $H_d(t) = \epsilon[a \exp(i\omega_c t) + a^\dagger \exp(-i\omega_c t)]$ . We numerically simulate the quantum evolution of the system described by the Lindblad-type master equation

$$\begin{aligned} \frac{d\rho(t)}{dt} = & -i[H_1 + H_d(t), \rho(t)] + \Gamma D[\sigma_-]\rho(t) + \gamma D[a]\rho(t) \\ & + \kappa n_{\text{th}} D[b]\rho(t) + \kappa(n_{\text{th}} + 1) D[b^\dagger]\rho(t), \end{aligned} \quad (\text{S28})$$

where  $\Gamma$ ,  $\gamma$ , and  $\kappa$  are the decay rates for the qubit, optical resonator, and SAW resonator, respectively,  $n_{\text{th}}$  is the thermal phonon number, and  $D[A]\rho = (2A\rho A^\dagger - A^\dagger A\rho - \rho A^\dagger A)/2$  is the decoherence term in the Lindblad superoperator form. Note that we consider the original Hamiltonian  $H_1$ , given in Eq. (S4) (including the qubit degree of freedom), rather than the reduced UOM Hamiltonian  $H_s$ , given in Eq. (S14).

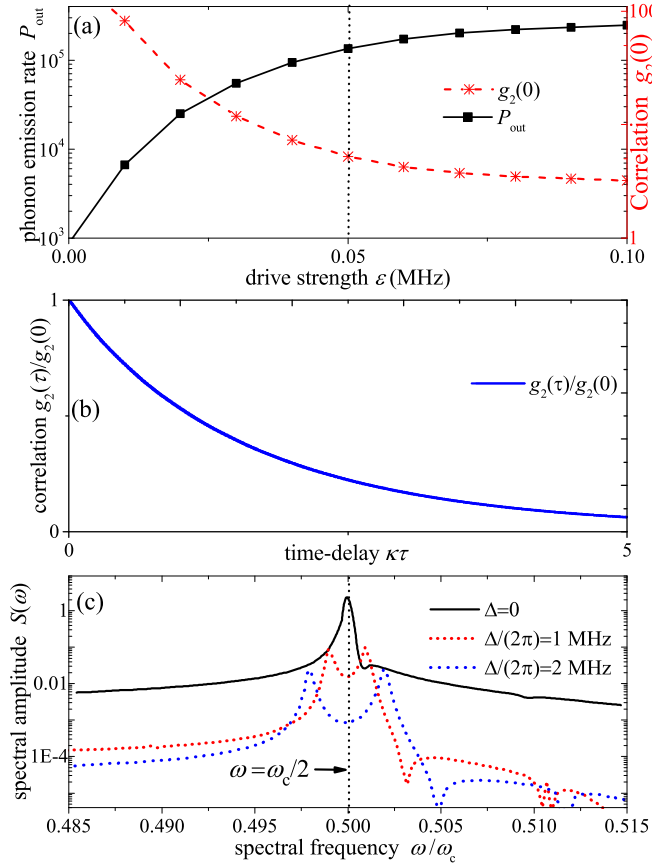


FIG. S2. (a) Phonon-output rate  $P_{\text{out}}$ , and correlation function  $g_2(0)$ , as functions of the TLR drive strength  $\epsilon$ . The dashed line is plotted at  $\epsilon/(2\pi) = 0.05$  MHz, which is set in plots (b) and (c). (b) Normalized correlation function  $g_2(\tau)/g_2(0)$  changing with the delay time  $\kappa\tau$ . (c) Phonon output spectrum density  $S(\omega)$ , for different detuning cases. The dotted line position corresponds to  $\omega = \omega_c/2$ . Here the decay rates are:  $\Gamma/(2\pi) = 0.05$  MHz,  $\kappa/(2\pi) = 0.2$  MHz, and  $\gamma/(2\pi) = 0.1$  MHz.

We first consider the SAW resonator coupled to a zero-temperature reservoir ( $n_{\text{th}} = 0$ ). As predicted in the optical DCE, with increasing the drive strength  $\epsilon$ , the effective length of the SAW resonator is modulated with a higher amplitude. In Fig. S2(a), by setting  $\omega_c = 2\omega_m$ , we plot the phonon output rate  $P_{\text{out}}$  changing with  $\epsilon$ . We find that, with large  $\epsilon$ ,  $P_{\text{out}}$  is enhanced. At  $\epsilon/(2\pi) = 0.05$  MHz (dashed line), the output phonon number per second is about  $P_{\text{out}} \simeq 1 \times 10^5$ , which can be effectively detected by an IDT measurement [S13].

Since there are no thermal excitations and no coherent drive applied to the SAW resonator, these phonons might be generated by the phonon DCE, and have the same quantum signatures as photons generated in the optical DCE. As discussed in Refs. [S24, S27], the DCE excitations are created in pairs. To show this, in Fig. S2(a), we plot the second-order correlation function  $g_2(0)$  as a function of the TLR drive strength  $\epsilon$ . We find that the generated phonons have super-Poissonian phonon-number statistics with  $g_2(0) \gg 2$ . When  $\epsilon$  has ultralow amplitude,  $g_2(0)$  becomes infinitely large [S23]. Due to the increasing phonon intensity [S21],  $g_2(0)$  decreases with increasing the drive strength. Moreover, in Fig. S2(b), we plot the normalized correlation function  $g_2(\tau)/g_2(0)$  changing with the delay time  $\kappa\tau$ . We find that  $g_2(0) \gg g_2(\tau)$ , indicating that the emitted phonons exhibit strong bunching, which is due to the same mechanism as that in the optical DCE [S23].

In Fig. S2(c), we plot the spectrum density  $n_{\text{out}}(\omega)$  for different values of the detuning  $\Delta_d = \omega_c - 2\omega_m$ . When  $\Delta_d = 0$ , the phonon-flux density spectrum shows a single-peak at  $\omega = \omega_s/2$ . When  $\Delta_d \neq 0$  [Fig. S2(a)],  $n_{\text{out}}(\omega)$  shows a clearly symmetric bimodal spectrum at  $\omega'$  and  $\omega''$ , with  $\omega' + \omega'' = \omega_c$ , which is another strong indication of the phonon DCE [S28]. Compared with the resonance case, the correlated emitted phonon pairs are not degenerate any more, but distributed into two conjugate modes with different frequencies. When increasing the detuning  $\Delta_d$ , the peaks of two modes separate with larger distance, while the amplitudes are suppressed significantly.

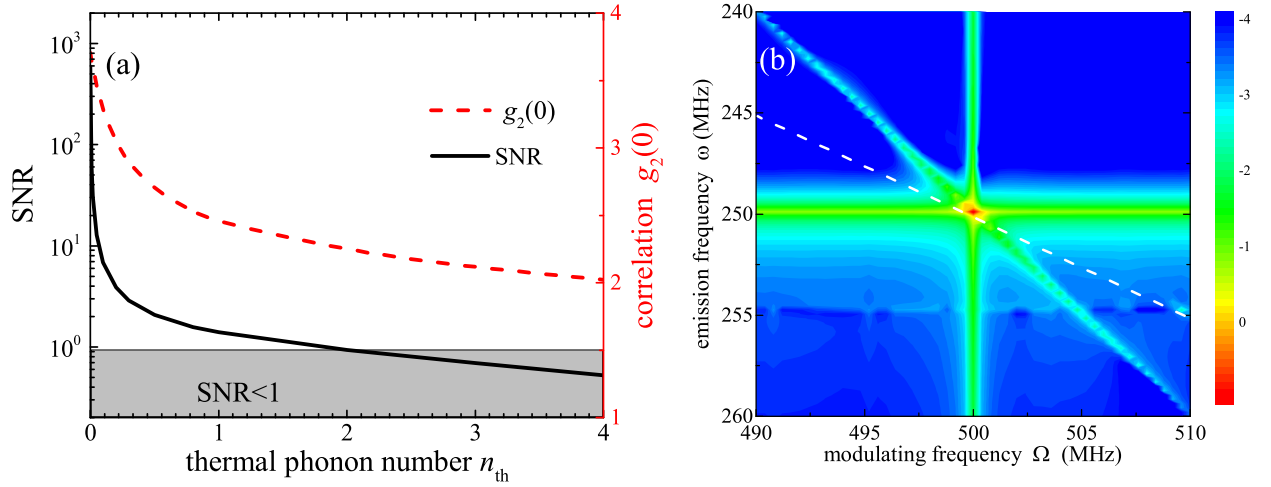


FIG. S3. (a) Signal-to-noise-ratio (SNR) and second-order correlation function  $g_2(0)$  versus the thermal phonon number  $n_{\text{th}}$ . The grey area corresponds to  $\text{SNR} < 1$ . (b) The emitted phonon spectrum  $\log[S(\omega)]$  changes with the modulating frequency  $\Omega$ . A bimodal spectrum structure distributes along the dashed line (which corresponds to  $\omega = \Omega/2$ ). Here we set the coherent drive amplitude on the qubit as  $\Omega_d/(2\pi) = 100$  MHz. Other parameters are the same as those in Fig. S2.

As discussed in Sec. II, the TLR can be replaced by a 1D transmission waveguide, which can support a classical drive current. Equations (S24) and (S25) indicate that the pulse shape in the waveguide directly determines how the effective phonon resonator length changes with time. We consider a simple case where a sinusoidal current pulse  $I(t) = \Theta(t)I_c \cos(\Omega t)$  is applied, which is equal to a coherent drive on the qubit operator  $\sigma_z$  with strength  $\Omega_d = g_z I_c / I_0$ . Following Eq. (S25), the current produces a time-dependent modulation of the effective phonon resonator length

$$\delta L(t) = \frac{4g_x^2}{\omega_q^2} \frac{\Omega_d}{\omega_m} L_0 \cos(\Omega t). \quad (\text{S29})$$

The sinusoidal modulation can be mapped as *moving a phonon mirror with a non-uniform acceleration* [S29]. Similarly, we can observe the *phonon DCE*. In the following, we consider how a non-zero temperature phonon reservoir influencing the *phonon DCE* signals.

Once considering these thermal effects, the emitted phonons from the SAW resonator can be divided into two parts: the DCE-induced phonon pairs and thermalized incoherent phonons. One can define the DCE signal-to-noise-ratio (SNR) as

$$\text{SNR} = \frac{P_{\text{out}} - P_{\text{out}}^{\text{th}}}{P_{\text{out}}^{\text{th}}}, \quad (\text{S30})$$

where  $P_{\text{out}}^{\text{th}}$  is the output *phonon* rate without modulating effective resonator length, while  $P_{\text{out}}$  is the total output phonon rate. Therefore,  $P_{\text{out}}^{\text{th}}$  corresponds to purely thermal excitations and should be considered as a noise

contribution. In Fig. S3(a), by setting  $\Omega = 2\omega_m$ , we plot the SNR and  $g_2(0)$  change with the thermal phonon number  $n_{\text{th}}$ . By increasing the thermal noise, the SNR decreases quickly. When  $n_{\text{th}} > 2$ , the SNR is below 1, indicating that the DCE signal would be hidden in the noisy background. Consequently, the second-order correlation  $g_2(0)$  decreases due to incoherent thermal emissions.

In Fig. S3(b), by setting  $n_{\text{th}} = 0.02$ , we plot the emission spectrum  $S(\omega)$  changing with the coherent modulation frequency  $\Omega$ . The dashed line position is plotted for  $\omega = \Omega/2$ . The bimodal structure of the emission spectrum is still kept. However, due to thermal noise, the two peaks are not symmetric any more. To suppress the effect of thermal noise on the DCE signals, one can employ high-frequency modes of the SAW cavity. As discussed in the experiments reported in Refs. [S11–S13], the SAW resonance frequency can be engineered for about several GHz, and the thermal occupation number  $n_{\text{th}}$  can be below  $10^{-3}$  at temperatures  $\sim 20$  mK, which is within the capability of up-to-date hybrid quantum circuit implementations in dilution refrigerators.

- 
- [S1] Y.-X. Liu, C.-X. Yang, H.-C. Sun, and X.-B. Wang, “Coexistence of single- and multi-photon processes due to longitudinal couplings between superconducting flux qubits and external fields,” *New J. Phys.* **16**, 015031 (2014).
  - [S2] Y. J. Zhao, Y. L. Liu, Y. X. Liu, and F. Nori, “Generating nonclassical photon states via longitudinal couplings between superconducting qubits and microwave fields,” *Phys. Rev. A* **91**, 053820 (2015).
  - [S3] S. Richer and D. DiVincenzo, “Circuit design implementing longitudinal coupling: A scalable scheme for superconducting qubits,” *Phys. Rev. B* **93**, 134501 (2016).
  - [S4] S. Richer, N. Maleeva, S. T. Skacel, I. M. Pop, and D. DiVincenzo, “Inductively shunted transmon qubit with tunable transverse and longitudinal coupling,” *Phys. Rev. B* **96**, 174520 (2017).
  - [S5] N. Didier, J. Bourassa, and A. Blais, “Fast quantum nondemolition readout by parametric modulation of longitudinal qubit-oscillator interaction,” *Phys. Rev. Lett.* **115**, 203601 (2015).
  - [S6] D. Zueco, G. M. Reuther, S. Kohler, and P. Hänggi, “Qubit-oscillator dynamics in the dispersive regime: Analytical theory beyond the rotating-wave approximation,” *Phys. Rev. A* **80**, 033846 (2009).
  - [S7] S.-Q. Ding, G. Maslennikov, R. Häblützel, and D. Matsukevich, “Cross-Kerr nonlinearity for phonon counting,” *Phys. Rev. Lett.* **119**, 193602 (2017).
  - [S8] W. J. Munro, K. Nemoto, R. G. Beausoleil, and T. P. Spiller, “High-efficiency quantum-nondemolition single-photon-number-resolving detector,” *Phys. Rev. A* **71**, 033819 (2005).
  - [S9] X. Gu, A. F. Kockum, A. Miranowicz, Y.-X. Liu, and F. Nori, “Microwave photonics with superconducting quantum circuits,” *Phys. Rep.* **718–719**, 1 (2017).
  - [S10] M. J. A. Schuetz, E. M. Kessler, G. Giedke, L. M. K. Vandersypen, M. D. Lukin, and J. I. Cirac, “Universal quantum transducers based on surface acoustic waves,” *Phys. Rev. X* **5**, 031031 (2015).
  - [S11] R. Manenti, M. J. Peterer, A. Nersisyan, E. B. Magnusson, A. Patterson, and P. J. Leek, “Surface acoustic wave resonators in the quantum regime,” *Phys. Rev. B* **93**, 041411 (2016).
  - [S12] R. Manenti, A. F. Kockum, A. Patterson, T. Behrle, J. Rahamim, G. Tancredi, F. Nori, and P. J. Leek, “Circuit quantum acoustodynamics with surface acoustic waves,” *Nat. Commun.* **8** (2017).
  - [S13] A. N. Bolgar, J. I. Zotova, D. D. Kirichenko, I. S. Besedin, A. V. Semenov, R. S. Shaikhaidarov, and O. V. Astafiev, “Quantum regime of a two-dimensional phonon cavity,” *Phys. Rev. Lett.* **120**, 223603 (2018).
  - [S14] A. F. Kockum, G. Johansson, and F. Nori, “Decoherence-free interaction between giant atoms in waveguide quantum electrodynamics,” *Phys. Rev. Lett.* **120**, 140404 (2018).
  - [S15] E. K. Irish and K. Schwab, “Quantum measurement of a coupled nanomechanical resonator–Cooper-pair box system,” *Phys. Rev. B* **68**, 155311 (2003).
  - [S16] C. P. Sun, L. F. Wei, Yu-xi Liu, and F. Nori, “Quantum transducers: Integrating transmission lines and nanomechanical resonators via charge qubits,” *Phys. Rev. A* **73**, 022318 (2006).
  - [S17] E. A. Sete, J. M. Martinis, and A. N. Korotkov, “Quantum theory of a bandpass purcell filter for qubit readout,” *Phys. Rev. A* **92**, 012325 (2015).
  - [S18] E. Sánchez-Burillo, L. Martín-Moreno, J. J. García-Ripoll, and D. Zueco, “Full two-photon down-conversion of a single photon,” *Phys. Rev. A* **94**, 053814 (2016).
  - [S19] C. K. Law, “Interaction between a moving mirror and radiation pressure: A Hamiltonian formulation,” *Phys. Rev. A* **51**, 2537 (1995).
  - [S20] J. J. Viennot, X. Ma, and K. W. Lehnert, “Phonon-number-sensitive electromechanics,” *Phys. Rev. Lett.* **121**, 183601 (2018).
  - [S21] V. Macrì, A. Ridolfo, O. Di Stefano, A. F. Kockum, F. Nori, and S. Savasta, “Nonperturbative dynamical Casimir effect in optomechanical systems: Vacuum Casimir-Rabi splittings,” *Phys. Rev. X* **8**, 011031 (2018).
  - [S22] J. R. Johansson, G. Johansson, C. M. Wilson, and F. Nori, “Dynamical Casimir effect in a superconducting coplanar waveguide,” *Phys. Rev. Lett.* **103**, 147003 (2009).
  - [S23] J. R. Johansson, G. Johansson, C. M. Wilson, and F. Nori, “Dynamical Casimir effect in superconducting microwave circuits,” *Phys. Rev. A* **82**, 052509 (2010).
  - [S24] C. M. Wilson, G. Johansson, A. Pourkabirian, M. Simoen, J. R. Johansson, T. Duty, F. Nori, and P. Delsing, “Observation

- of the dynamical Casimir effect in a superconducting circuit,” *Nature (London)* **479**, 376 (2011).
- [S25] Y.-X. Liu, A. Miranowicz, Y. B. Gao, J. Bajer, C. P. Sun, and F. Nori, “Qubit-induced phonon blockade as a signature of quantum behavior in nanomechanical resonators,” *Phys. Rev. A* **82**, 032101 (2010).
- [S26] M. O. Scully and M. S. Zubairy, *Quantum Optics* (Cambridge University Press, Cambridge, 1997).
- [S27] P. Lähteenmäki, G. S. Paraoanu, J. Hassel, and P. J. Hakonen, “Dynamical Casimir effect in a Josephson metamaterial,” *PNAS* **110**, 4234 (2013).
- [S28] A. Lambrecht, M. Jaekel, and S. Reynaud, “Motion induced radiation from a vibrating cavity,” *Phys. Rev. Lett.* **77**, 615 (1996).
- [S29] P. D. Nation, J. R. Johansson, M. P. Blencowe, and F. Nori, “Colloquium: Stimulating uncertainty: Amplifying the quantum vacuum with superconducting circuits,” *Rev. Mod. Phys.* **84**, 1 (2012).